

1 Article

2 Susceptibility of *Exopalaemon carinicauda* to the 3 infection with Shrimp hemocyte iridescent virus

4 Xing Chen ^{1,2}, Liang Qiu ¹, Hailiang Wang ¹, Peizhuo Zou ¹, Xuan Dong ¹, Fuhua Li ³, Jie Huang ^{1,2*}

5 1. Yellow Sea Fisheries Research Institute, Chinese Academy of Fishery Sciences; Laboratory for Marine
6 Fisheries Science and Food Production Processes, National Laboratory for Marine Science and Technology
7 (Qingdao); Key Laboratory of Maricultural Organism Disease Control, Ministry of Agriculture and Rural
8 Affairs; Qingdao Key Laboratory of Mariculture Epidemiology and Biosecurity; Qingdao 266071, China

9 2. Shanghai Ocean University, Shanghai 201306, China

10 3. Key Laboratory of Experimental Marine Biology, Institute of Oceanology, Chinese Academy of Sciences,
11 Qingdao, 266071, China.

12 * Correspondence: huangjie@ysfri.ac.cn

13

14 **Abstract:** In this study, ridgetail white prawns *Exopalaemon carinicauda* were infected *per os* with
15 debris of Shrimp hemocyte iridescent virus (SHIV)-infected *Penaeus vannamei* and via intramuscular
16 injection (im) with raw extracts of SHIV. The infected *E. carinicauda* showed obvious clinical
17 symptoms, including weakness, empty gut and stomach, pale hepatopancreas, and partial death
18 with cumulative mortality of (50.0±26.5)% and (76.7±18.3)%, respectively. Results of TaqMan probe
19 based real-time quantitative PCR showed that the moribund and survival individuals with clinical
20 signs of infected *E. carinicauda* were SHIV-positive. Histological examination showed that there
21 were dark eosinophilic inclusions, of which some were surrounded with or contained tiny
22 basophilic staining, and pyknosis in cytoplasm of hemocytes in the hepatopancreatic sinus,
23 hematopoietic cells, and cuticular epithelium, etc. Positive hybridization signals were observed in
24 stomach, hematopoietic tissue, cuticular epithelium, and hepatopancreatic sinus of infected prawns
25 from both *per os* and im groups, according to the results of *in situ* DIG-labeling-loop-mediated DNA
26 Amplification (ISDL). Transmission electron microscopy of ultrathin sections showed that
27 icosahedral SHIV particles existed in hepatopancreatic sinus and gills of the infected *E. carinicauda*
28 of the *per os* group. The viral particles were also observed in the hepatopancreatic sinus, gills,
29 pereopods, muscles, and uropods of the infected *E. carinicauda* from the im group. The assembled
30 virions mostly distributed outside of the assembling area near cellular membrane of infected cells,
31 which were with envelope and about 150 nm in diagonal diameter. The results of molecular
32 biological tests, histopathological examination, ISDL, and transmission electron microscopy
33 confirmed that *E. carinicauda* is one of the susceptible hosts of SHIV. This study also reminded that
34 *E. carinicauda* showed some degree of tolerance to the infection with SHIV *per os* challenge
35 mimicking natural pathway.

36

37 **Keywords:** Shrimp hemocyte iridescent virus; *Exopalaemon carinicauda*; susceptibility; host; ISDL

38

39 1. Introduction

40 The iridescent virus family *Iridoviridae* contains large icosahedral double-stranded DNA viruses,
41 which is divided into two subfamilies (i.e., *Alphairidovirinae* and *Betairidovirinae*) and composed of
42 five known genera: *Lymphocystivirus*, *Megalocytivirus*, *Ranavirus*, *Chloriridovirus*, and *Iridovirus*. Of
43 them, the genera *Lymphocystivirus*, *Megalocytivirus*, and *Ranavirus* belong to *Alphairidovirinae*, and

44 *Chloriridovirus* and *Iridovirus* belong to *Betairidovirinae* [1-3]. Iridescent viruses of *Alphairidovirinae* lead
45 a high mortality rate in significant fish and amphibians [3], While iridescent viruses *Betairidovirinae*
46 infect insects and crustaceans. The first discovery of a possible iridescent virus in crustaceans was
47 published in 1993 [4]. In the same year Lightner and Redman reported the observation of another
48 suspected iridescent virus in Penaeid shrimp *Protrachypene precipua* [5]. Subsequently, Miao et al.
49 reported that a suspected iridescent virus observed in lymphoid cell cultures on *Penaeus chinensis* in
50 1999 [6]. Years later, Tang et al. (2007) identified an iridovirus, i.e., Sergestid iridovirus (SIV), from
51 diseased sergestid shrimp *Acetes erythraeus*, which is a likely causative agent, evidenced through *in*
52 *situ* hybridization and PCR test [7]. Xu et al. (2016) reported *Cherax quadricarinatus* iridovirus (CQIV)
53 isolated from diseased red claw crayfish *Cherax quadricarinatus* [8]. Qiu et al (2017) identified an
54 iridescent virus named Shrimp hemocyte iridescent virus (SHIV), which isolated from farmed *Penaeus*
55 *vannamei* in 2014 and also detected in *P. chinensis* and *Macrobrachium rosenbergii* [9].

56 The range of susceptible hosts is an important part of epidemiology and pathogen ecology. It is
57 also highly concerned for international trade and control of the disease. The World Organisation for
58 Animal Health (OIE) has adopted a chapter in “The Aquatic Animal Health Code” to provide criteria
59 for determining which species are listed as susceptible in 2014 with emphasis that the route of
60 transmission is consistent with natural pathways for the infection [10]. Ridgetail white prawn
61 *Exopalaemon carinicauda* is one of major economic crustaceans in China, which could propagate
62 throughout all the year round, naturally distributes in the coast of Yellow Sea and Bohai Sea of China
63 [11,12]. *E. carinicauda* accounts for one third of the total yields of polyculture ponds in the eastern
64 China [11]. It is also a species of wild prawn and commonly exists in the ponds farming *M. rosenbergii*
65 or penaeid shrimp. To date, there is no report pointing out that *E. carinicauda* can be infected with
66 iridescent viruses. Owing to the common existence in intensive prawn farming ponds, it is important
67 for precaution of the spreading risk of SHIV, which is based on assessing the susceptibility of *E.*
68 *carinicauda* to SHIV and evaluating SHIV potential transmission routes and possible reservoirs in the
69 nature. In this study, *E. carinicauda* were challenged *per os* to mimic natural infection according to the
70 OIE standards, while intramuscular injection was used as a positive control. A combination of
71 TaqMan real-time PCR, histopathological observation, *in situ* DIG-labeling-loop-mediated DNA
72 amplification (ISDL) and ultra-thin transmission electron microscopy were used to confirm the
73 infection with SHIV in *E. carinicauda*.

74 2. Materials and Methods

75 2.1. Animals

76 Specific-pathogen-free (SPF) ridgetail white prawns *E. carinicauda*, (7.2±0.5) cm in body length,
77 were reared and bred in the Key Laboratory of Experimental Marine Biology, Institute of Oceanology,
78 Chinese Academy of Sciences. Prawns *E. carinicauda* were cultivated in a 40 L plastic tanks containing
79 20 L seawater of 30 ppt in salinity with 90% daily exchange rate, at 27 °C water temperature, with
80 continuous aeration, and fed three times per day with the formula feed for a week in our wet lab. For
81 multiplication of SHIV, 30 healthy white leg shrimp *P. vannamei* of (10.2±0.8) cm in body length were
82 purchased from a shrimp farm in Weifang of Shandong Province and then held in 40 L of 30 ppt
83 salinity seawater with same management above mentioned.

84 Before challenge test, the prawns and the shrimp were sampled and detected for potential
85 pathogens, including White spot syndrome virus (WSSV), Taura syndrome virus (TSV), Yellow head
86 virus (YHV), Infectious hypodermal and hematopoietic necrosis virus (IHHNV), and acute
87 hepatopancreatic necrosis disease-causing *Vibrio parahaemolyticus* (*Vp*_{AHPND}), using the nested PCR or
88 TaqMan probe based quantitative real-time PCR (TaqMan qPCR) methods [13], Covert mortality
89 nodavirus (CMNV) using TaqMan qPCR methods [14], and SHIV using nested PCR [15].

90 2.2. Preparation of Viral Inoculum

91 For preparation of material for challenge test, 30 healthy shrimp *P. vannamei* were infected by
92 feeding with SHIV (strain 20141215) infected tissue, which was derived from diseased *P. vannamei*

93 collected in a farm in Zhejiang Province in Dec. 2014 [9]. After 5 days post-infection, 2.5 g
94 cephalothoraxes (removing tergites) were taken from SHIV-infected shrimp and subsequently
95 homogenized in 40 mL pre-cooled PPB-Tris (376.07 mM NaCl, 6.32 mM K₂SO₄, 6.4 mM MgSO₄, 14.41
96 mM CaCl₂, and 50 mM Tris-HCl, pH 6.5–8.0) [16]. The suspension was centrifuged at 10,000 rpm for
97 10 min at 4 °C. The pellet was resuspended in 25 mL PPB-Tris by homogenization and re-centrifuged.
98 The supernatants from two steps were merged and filtered through a 500-mesh sieve and a 0.45 µm
99 filter. SHIV dose in the suspension was quantified using TaqMan qPCR method [15]. For challenge
100 test via intramuscular injection, an inoculum containing 10⁴ copies/µL SHIV was prepared by diluting
101 the suspension with PPB-His (replace 50 mM Tris-HCl with 50 mM Histidine in PPB-Tris) [16], and
102 then the inoculum was dispensed in 100 µL aliquots before stored at –80 °C.

103 2.3. Challenge Tests

104 Challenge tests were performed with healthy *E. carinicauda* in 4 groups, including intramuscular
105 injection (IM), *per os* (PO), control of intramuscular infection (CIM), and control of *per os* (CPO). Each
106 group had 3 replicates with 10 prawn individuals per replicate. Each prawn in the IM group was
107 injected 10 µL of viral inoculum (~10⁵ copies). Prawns in the PO group were fed with total 3 g debris
108 of SHIV-infected *P. vannamei* tissue (with a viral dose about 10¹⁰ copies/g). Prawns in the CIM group
109 and the CPO group were injected with 10 µL sterile PPB-His and commercial formula feed,
110 respectively. During the test period, the rearing conditions were kept as same as that prior to
111 challenge.

112 Significance analysis of cumulative mortalities between each two groups was carried out using
113 the t-test for homoscedasticity hypothesis of two group samples with the add-in tool of Data Analysis
114 in Microsoft® Excel® 2016 MSO 64-bit.

115 For evaluation of the pathogenic model in the infection groups, mortality data were nonlinearly
116 regressed following 3-parameter sigmoid equation: $M(t) = \frac{a}{1+e^{-k(t-t_0)}}$, of which $M(t)$ is the cumulative
117 mortality at the time (day post infection); t is the time (day post infection); a is the maximum mortality;
118 t_0 is the day post infection to the half of the maximum mortality; k is the instant incidence rate. The
119 real pathogenic model shall deduct the average mortality of control groups.

120 2.4. Detection of SHIV Using TaqMan Probe Based Real-Time Quantitative PCR

121 Total DNA were extracted from the hepatopancreas of samples stored at -20 °C using a
122 TIANamp Marine Animals DNA Kit (Tiangen, Beijing, China), respectively. TaqMan qPCR, using
123 the total DNA samples as templates, was conducted as described previously [15] to detect and
124 quantify SHIV. The forward and reverse primers were SHIV-F 5'-AGG AGA GGG AAA TAA CGG
125 GAA AAC-3' and SHIV-R 5'-CGT CAG CAT TTGGTT CAT CCA TG-3', respectively. The TaqMan
126 probe (5'-CTG CCC ATC TAA CAC CAT CTC CCG CCC-3') was labeled with 5'-6-carboxyfluorescein
127 (FAM) and 3'-TAMRA. Each PCR mixture in 20 µL contained 10 µL 2× FastStart Essential DNA
128 Probes Master (Roche, Indianapolis, IN, USA), 500 nM primer each, 200 nM probe, 100 ng total DNA
129 template. The program was initial denaturation at 95 °C for 10 min, following 40 cycles at 95 °C for
130 10 s and 60 °C for 30 s. The amplification and data analysis were carried out in a CFX-96 Quantitative
131 Fluorescence Instrument (BioRad, USA).

132 2.5. Histopathological Examination

133 The cephalothoraxes of *E. carinicauda*, sampled during the challenge tests, were fixed with
134 Davison's AFA fixative (DAFA) for 24 h and processed for sectioning and hematoxylin and eosin
135 (H&E) staining as described by Bell & Lightner [17]. The histological sections were analyzed and
136 photographed under a light microscopy system (Eclipse 80i, Nikon, Japan).

137 2.6. Loop-mediated Isothermal Amplification (LAMP)

138 A set of specific primers, composed of FIP, BIP, LF, LB, F3, and B3, for LAMP detection of SHIV
139 was designed targeting the gene of DNA-directed RNA polymerase II second largest subunit of SHIV

140 genomic sequence (GenBank accession No. MF599468), using PrimerExplorerV4
141 (<http://primerexplorer.jp/elamp4.0.0/index.html>). These primers were searched against the database
142 in NCBI (<http://blast.ncbi.nlm.nih.gov/Blast.cgi>) to analyze the sequence similarities. The primers
143 were synthesized by Sangon Biotech (Shanghai, China). Each LAMP mixture contained 1.6 μ M each
144 of inner primers FIP and BIP, 0.8 μ M each of loop primers LF and LB, 0.2 μ M each of outer primers
145 F3 and B3, 1.4 mM of dNTP mix (TaKaRa, Dalian, China), 1.2 M betaine (Solarbio, Beijing, China), 25
146 μ M calcein (Sigma, USA), 500 μ M MnCl₂, 6 mM MgCl₂, 8 U Bst 2.0 DNA polymerase (New England
147 Biolabs Inc., Beverly, USA), 1 \times supplied buffer and the specified amount of template DNA in a final
148 volume of 25 μ L. The procedure was 60 cycles for 60 °C, following 5 minutes at 85 °C on the CFX-96
149 Quantitative Fluorescence Instrument (BioRad, USA) using calcein fluorescent channel. Detection
150 specificity of the LAMP primers were examined using 100 ng of total DNA extracted from uninfected
151 prawns and shrimp infected with other pathogens, including WSSV, *Vp_{AHPND}*, IHNV, and EHP.

152 2.7. *In situ* DIG-labeling-loop-mediated DNA Amplification (ISDL)

153 ISDL followed the method published by Jitrakorn et al. [18] with some modification to target
154 SHIV. Paraffin sections were dewaxed and rehydrated according to the normal DIG-labeled *in situ*
155 hybridization method [17-19]. Rehydrated slides were added with ddH₂O and denatured on a 100 °C
156 heating block for 2 min, then subsequently placed in a wet box. Total 150 μ L LAMP mixture, of which
157 the components are as same as 2.6, above except that the dNTP mix was supplemented with 0.1 mM
158 digoxigenin-11-dUTP (DIG-labeled dUTP) and without calcein and MnCl₂, were added dropwise to
159 each slide. The mixture was incubated at 65 °C for 60 min, followed by 85 °C for 5 min. Subsequent
160 steps were performed in accordance with a normal *in situ* hybridization [19]. Tissue sections of
161 healthy prawns were used as the control.

162 2.8. Ultrathin Transmission Electron Microscopy

163 For transmission electron microscopy with ultrathin sections, samples were prepared as
164 previous described [20,21]. Briefly, tissues of hepatopancreas, muscle, pereopods, uropods, and gills
165 of infected *E. carinicauda* were placed in TEM fixative (2% paraformaldehyde, 2.5% glutaraldehyde,
166 160 mM NaCl and 4 mM CaCl₂ in 200 mM PBS, pH 7.2) and cut rapidly into ~ 1 mm³ pieces with
167 scalpels, fixed for 1 h at room temperature, and then post-fixed with OsO₄. Specimens were
168 embedded in Spurr's plastic and dyed with uranyl acetate and lead citrate. Ultrathin sections were
169 prepared on collodion-coated grids by the Equipment Center of the Medical College, Qingdao
170 University (Qingdao, China). All grids were examined under a JEM-1200 electron microscope (JEOL,
171 Japan) operating at 80–100 kV.

172 3. Results

173 3.1. Clinical Signs and Cumulative Mortality

174 The challenge test lasted for 15 days. After 3 days post infection (dpi), prawns in both
175 intramuscular (IM) and *per os* (PO) groups were clinically infected, which displayed empty stomach
176 and gut and pale hepatopancreas, the hematopoietic tissue under the base of rostrum showed slight
177 white color (Figure 1, IM and PO); while prawns in the control groups (i.e., CPO and CIM) displayed
178 normal gross signs, including feed-filled stomach and gut and light brown hepatopancreas, but the
179 hematopoietic tissue was not visible (Figure 1, CPO).

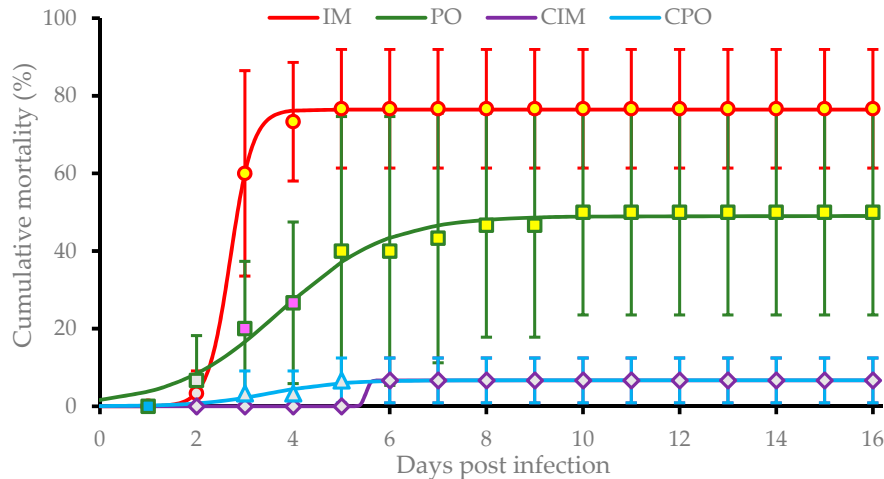


180

181 **Figure 1.** Gross signs of prawns *Exopalaemon carinicauda* in different groups of the challenge test. **CPO:**
 182 Prawn in *per os* control group; **PO:** Prawn in *per os* group; **IM:** Prawn in intermuscular injection group.
 183 Solid arrows indicate stomach (ST), hepatopancreas (HP), midgut (MG), and hematopoietic tissue
 184 (HM). Red bar = 10 mm.

185 Prawns in IM and PO groups suffered from rapid increasing of mortalities during the period
 186 between 2 dpi and 5 dpi. The average cumulative mortalities stabilized at (76.7±18.3)% and
 187 (50.0±26.5)% in the IM group after 5 dpi and PO group after 10 dpi, respectively, which were both
 188 significantly higher ($P < 0.01$) than that of CIM and CPO groups. Additionally, the cumulative
 189 mortality of the IM group was significantly higher ($P < 0.05$) than that of the PO group at 3 dpi and 4
 190 dpi (Figure 2). Significance analysis of the overall data of four groups showed very significant
 191 differences among IM, PO, and control groups ($P < 0.01$).

192 Based on the nonlinear regression following the 3-parameter sigmoid equation, the pathogenic
 193 model of infection with SHIV on *E. carinicauda* via im and *per os* were $M_{IM(t)} = \frac{70.77 \pm 0.21}{1 + e^{-(4.76 \pm 2.49)[t - (2.64 \pm 0.21)]}}$
 194 and $M_{PO(t)} = \frac{42.52 \pm 1.22}{1 + e^{-(0.82 \pm 0.51)[t - (3.83 \pm 0.87)]}}$, respectively. The functions indicated the infection of *E.*
 195 *carinicauda* with SHIV via im caused (70.77±0.21)% accumulative mortality, while the infection *per os*
 196 caused (42.52±1.22)% accumulative mortality. The former reached the half level of accumulative
 197 mortality in (2.64±0.21) dpi with an instant incidence rate at (4.76±2.49)/day; and the latter did in
 198 (3.83±0.87) dpi with an instant rate at (0.82±0.51)/day.

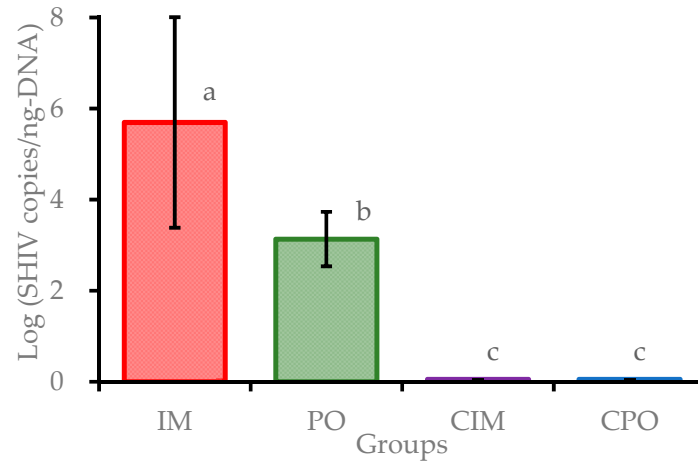


199

200 **Figure 2.** Cumulative mortalities of *Exopalaemon carinicauda* in the challenge test. IM group, prawns
 201 were challenged with filtrated viral suspension via intermuscular injection; PO group, prawns were
 202 fed with tissues of SHIV-infected *P. vannamei*; CIM group, prawns were injected with sterile PPB-His
 203 buffer; CPO group, prawns were fed with commercial feed. Cumulative mortalities are shown as
 204 means of data from 3 replicates for each experimental group (each replicate contained 10 individuals).
 205 The mean points with same color indicate no significant difference ($P > 0.05$), and the mean points with
 206 different colors indicate a significant difference ($P < 0.05$). Overall analysis indicated there are very
 207 significant differences among groups IM, PO, and the two controls ($P < 0.01$). The curves were drawn
 208 based on the nonlinear regression following the 3-parameter sigmoid equation.

209 3.2. TaqMan qPCR Detection

210 Moribund prawns in IM and PO groups were sampled for the experimental duration, and all
 211 the survival prawns in each group were collected at the end of the challenge experiment. All the
 212 prawn samples were detected for potential pathogens, using the TaqMan qPCR method. The SHIV-
 213 positive rates were 80.0% (24/30) and 46.7% (14/30) in the IM group and the PO group, respectively.
 214 The results showed that tests of SHIV were negative for the survival prawns in IM and PO groups.
 215 No SHIV positive was detected in CIM and CPO groups. The tests of Vp_{AHPND} , IHNV and WSSV
 216 were negative for all of prawn samples. The logarithmic SHIV loads (in copies/ng-DNA) of IM and
 217 PO group were 5.65 ± 2.31 , 3.08 ± 0.60 in prawns, respectively; while CIM and CPO groups were
 218 negative. The viral loads in challenged prawns in the IM group were significantly higher ($P < 0.01$)
 219 than that in the PO group (Figure 3). The loads of SHIV in 21 moribund and died prawns in the IM
 220 group were detected to reach $(4.20 \pm 3.88) \times 10^6$ copies/ng-DNA, while that in 3 non-clinical prawns
 221 were detected at only $(5.47 \pm 4.16) \times 10^{-1}$ copies/ng-DNA. The loads of SHIV in 7 died prawns in the PO
 222 group during 5 – 7 dpi averaged at $(3.63 \pm 1.44) \times 10^4$ copies/ng-DNA, which were much higher than
 223 that in 7 survival prawns in the same group at $(3.57 \pm 3.42) \times 10^2$ copies/ng-DNA (Figure S1). These
 224 results showed that prawns in IM and PO groups were successfully infected by SHIV.

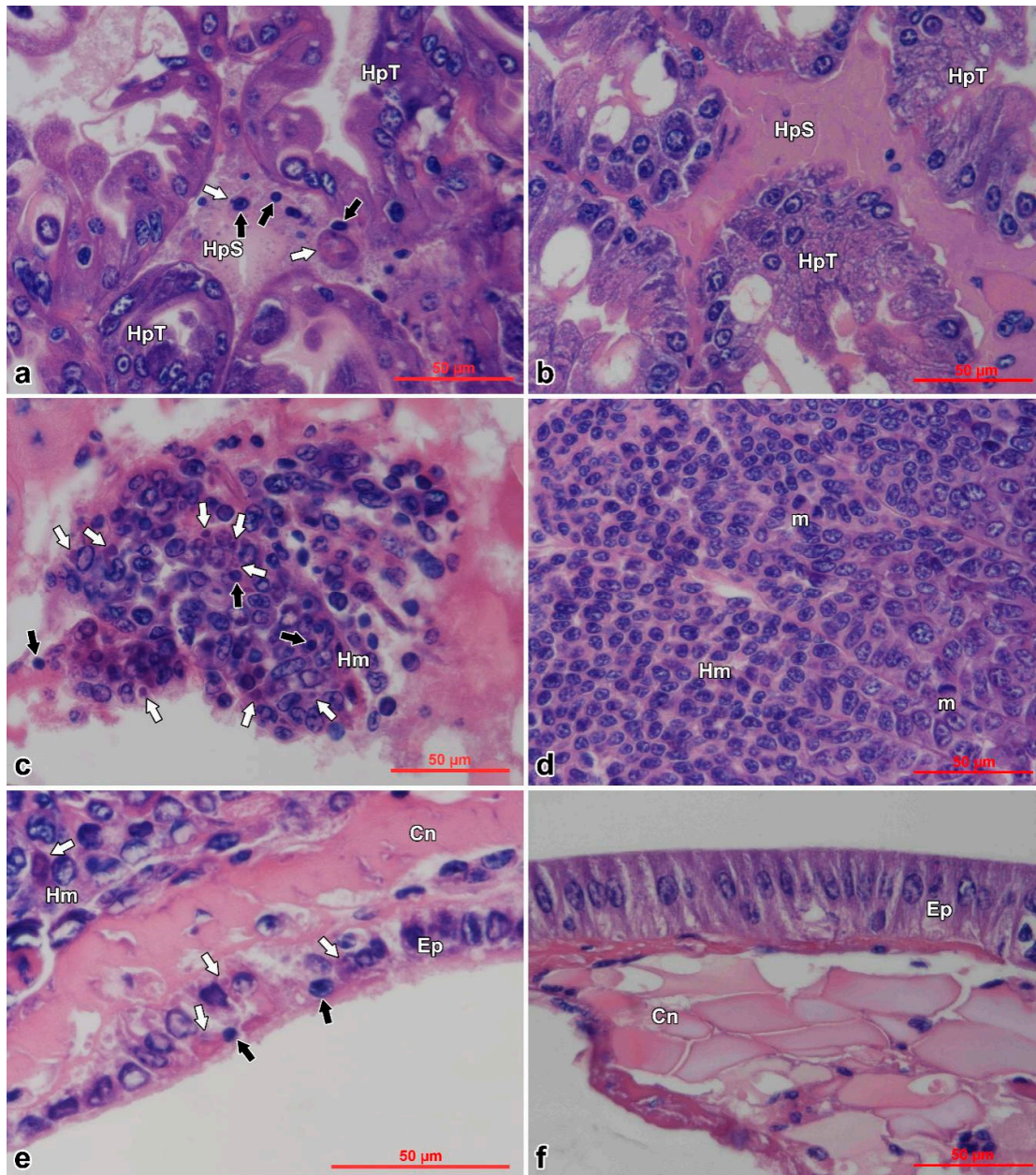


225

226 **Figure 3.** SHIV loads in prawns *Exopalaemon carinicauda* from the challenge test. Different letters above
227 the bars indicate significant difference ($P < 0.01$). CIM and CPO were negative.

228 3.3. Histopathology

229 Histopathological examination of moribund prawns showed that nuclear pyknosis and
230 acidophilic inclusions could be observed in the hemocytes of hepatopancreatic sinus (Figure 4a),
231 hemotoblasts of hematopoietic tissues (Figure 4c), and cuticular epithelium (Figure 4e); while the
232 tissues of the control prawns showed normal (Figure 4b, 4d, and 4f). Typical cytoplasmic and dark
233 eosinophilic inclusions, of which some were surrounded with or contained tiny basophilic staining,
234 appeared beside the nuclei in hematopoietic tissues, hemocytes, and epithelium. The inclusions were
235 more easily found in the infected hematopoietic tissues (Figure 4b).



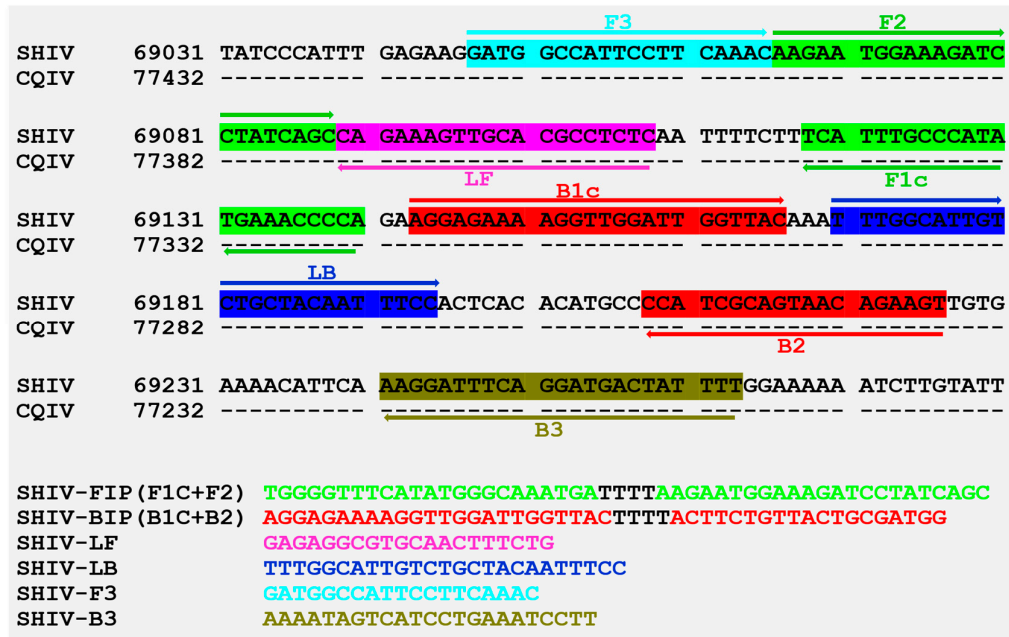
236

237 **Figure 4.** Histopathological examination of *E. carinicauda* tissues infected with SHIV and controls.
 238 Black arrows show the karyopyknosis and white arrows show the eosinophilic inclusions.
 239 Hepatopancreas (**a and b**); hematopoietic tissues (**c and d**), and cuticular epithelium (**e and f**) on which
 240 the cuticle were removed before dehydration. The left column (**a, c, and e**) are the tissues of the
 241 infected prawn; the right column (**b, d, and f**) are the tissues of the control prawn. HpT:
 242 hepatopancreatic tubule; HpS: hepatopancreatic sinus; Hm: haematopoietic tissue; Ep: epithelium;
 243 Cn: connective tissue; m: mitotic phase. Bar = 50 µm

244 3.4. Primer Design and LAMP Reaction

245 Primers for LAMP were designed targeting the gene of DNA-directed RNA polymerase II
 246 second largest subunit locating between 69047–69263 of SHIV genome (GenBank access no.
 247 MF599468), of which the sequence of was completely complementary to that of CQIV 77416–77200
 248 (Figure 5). In addition, results of LAMP primer specificity assay showed that the reactions were only
 249 positive for SHIV-infected shrimp, while the reactions were negative for WSSV, *Vp*_{AHPND}, IHNV or

250 EHP infected shrimp. It indicated that the LAMP primers in this study were specific to SHIV and
 251 should be available for ISDL.



252

253

254

Figure 5. Information of primer design and primers used for LAMP, based on the reference sequence of SHIV. Sequences of SHIV (MF599468) and CQIV (MF197913) were obtained from GenBank.

255

3.5. ISDL

256

257

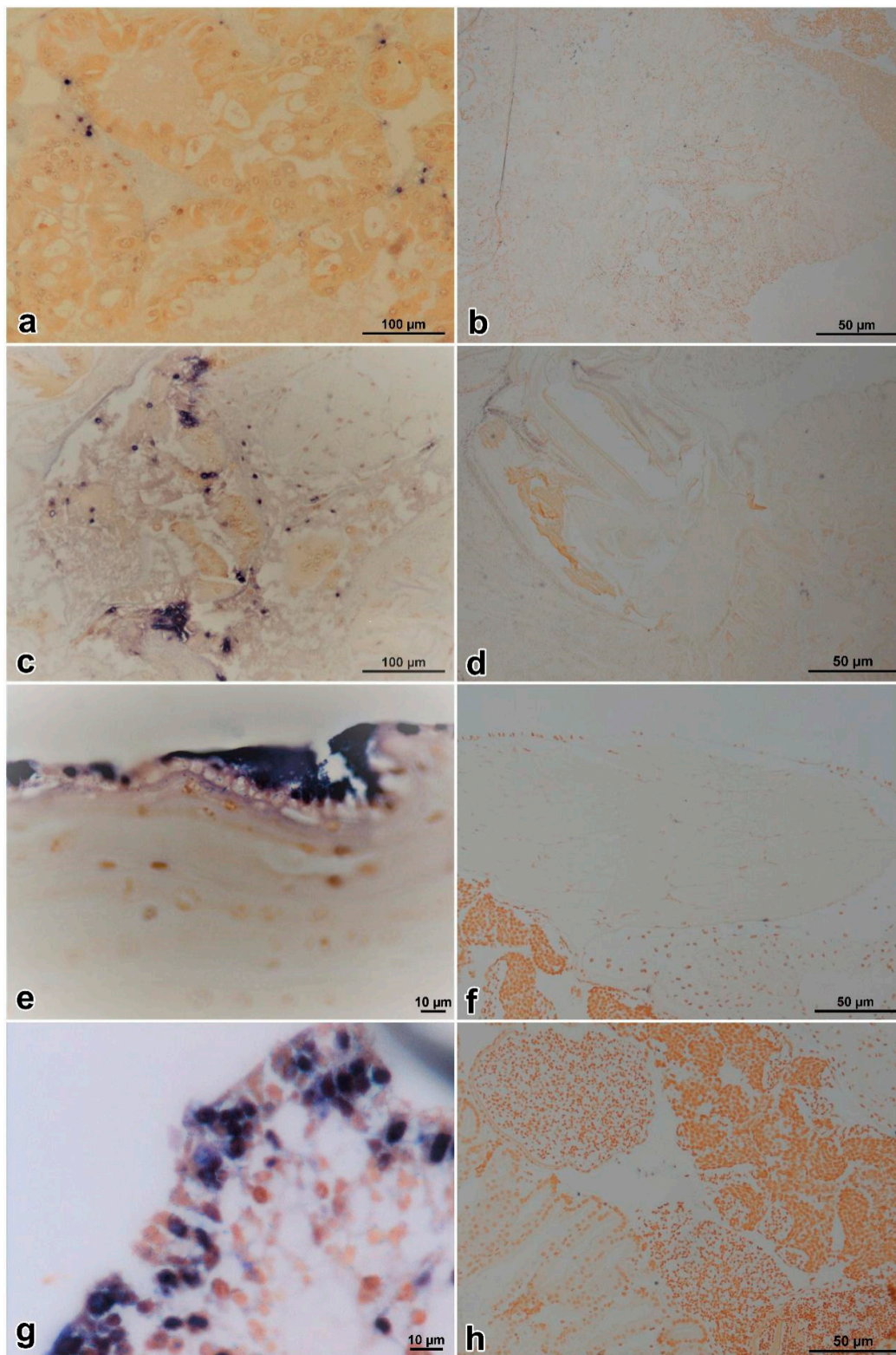
258

259

260

261

A LAMP system was applied to *in situ* hybridization, used to examine the histological sections. ISDL results showed that blue-violet hybridization signals were detected in the hepatopancreatic sinus, stomach epithelium, cuticular epithelium, and hematopoietic tissues (Figure 6a, 6c, 6e, and 6g) of prawns in the IM and PO groups, but no signal was detected in the control groups (Figure 6b, 6d, 6f, and 6h). The results of ISDL provided further evidences that prawns in IM and PO groups were infected by SHIV.



262

263

264

265

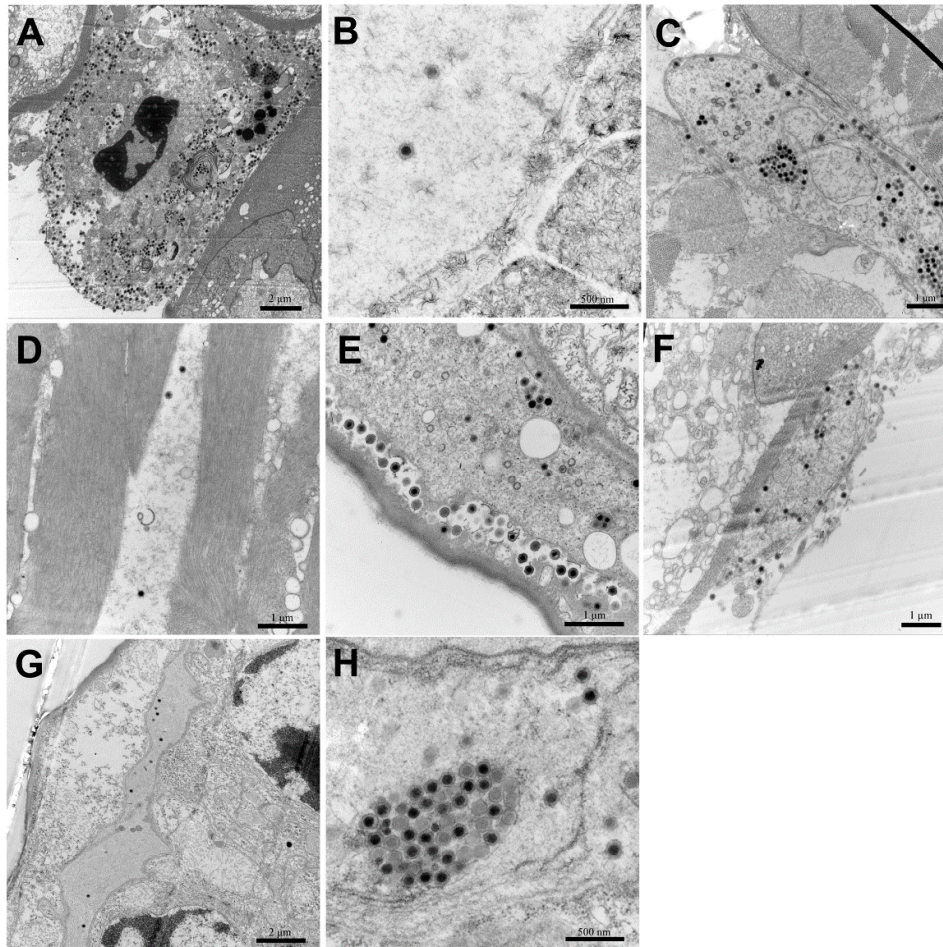
266

Figure 6. ISDL micrographs of diseased and healthy *E. carinicauda*. Hepatopancreas, stomach, cuticular epithelium, and hematopoietic tissue from a health prawn of PO group, respectively (a, c, e, and g); hepatopancreas, stomach, cuticular epithelium, and hematopoietic tissue from a diseased prawn of CPO group, respectively (b, d, f, and h).

267

3.6. TEM

268 Icosahedral virions and cytoplasmic inclusions were observed in hepatopancreatic sinus,
269 pereiopods, uropods, muscle and gills of *E. carinicauda* in the IM group (Figure 7A–7E, and 7H).
270 Assembled virions mostly distributed outside of the assembling area near cellular membrane of
271 infected cells (Figure 7A, E). Similarly, virions were observed in the hepatopancreatic sinus and gills
272 of prawns in the PO group (Figure 7F, G). Virions were hexagonal (i.e., icosahedral) and about 150
273 nm in diagonal diameter which matched with characteristics of SHIV.



274

275

276 **Figure 7.** Transmission electron microscopy (TEM) of diseased *E. carinicauda*. A–E: hepatopancreatic

277 sinus, pereiopods, uropods, muscle and gills, respectively, of a prawn in the IM group; F and G:

278 hepatopancreatic sinus and gills, respectively, of a prawn in the PO group; H: cytoplasmic inclusions

278 with a cluster of viral particles.

279

4. Discussion

280

281 Understanding the susceptibility of host range for a virus is important information for both

282 study on host and virus. On the host aspect, knowing an infectious pathogen of a host species will

283 provide important information for prevention of the relevant disease; on the virus aspect, the

284 information of a susceptible host range can be used for identification of virus species, finding of a

285 specific viral replication host or cell line, and understanding of viral ecology. Susceptible host range

286 also is important for international trade to prevent from the transboundary spreading of a specific

287 disease. For the purpose, OIE has issued criteria to determine susceptibility for a specific disease in

288 2014, which require evidences from either natural infection or experimental challenge mimicking

289 natural infection [10]. As a newly found virus, the susceptible host range of SHIV, including its

290 homologous strain named as CQIV sharing 99% genome similarity, remains large unknown space to

be investigated. For the natural infection pathway, Positive detections of SHIV by PCR or qPCR have

291 been reported in different natural samples of crustacean, including *P. vannamei* [9], *P. chinensis* [9], *M.*
292 *rosenbergii* [9,22], *C. quadricarinatus* [8], *Procambarus clarkii* [22,23], *P. japonicus* [22], *M. nipponense*
293 [22,23], *M. superbum* [23], and Cladocera [23]. Severe disease with high mortality has been reported
294 and infection with SHIV/CQIV has been demonstrated in *C. quadricarinatus*, *P. vannamei*, and *M.*
295 *rosenbergii* [8,9,23], these species are the confirmed susceptible species for SHIV/CQIV which concord
296 to the criteria of OIE standards for natural infection. Due to lack of the evidence for infection, usually
297 presented by histopathology, TEM, or *in situ* hybridization, only detected positives by PCR or qPCR
298 for SHIV cannot confirm the susceptibility of *P. chinensis*, *P. japonicus*, and *M. superbum* [22,23].
299 However, they may remain as suspicious susceptibility as there are confirmed susceptible species in
300 the same genus. Cladocera has been detected as positive by qPCR, but the ISDL result showed
301 negative. It has been considered as a non-susceptible species [23]. For the experimental infection
302 pathway, The experimental challenges of *P. vannamei*, *Pr. clarkii*, Chinese mitten crab *Eriocheir sinensis*,
303 and wild crab *Pachygrapsus crassipes* with CQIV have been reported [8,24]. Unfortunately, all of these
304 experimental infections used only intramuscular injection, the results were not enough to support
305 the confirmation of susceptibility for these species according to the criteria of OIE standards requiring
306 the challenge pathway mimicking natural infection. Our present study is the first report to confirm
307 susceptibility for the newly found virus by experimental pathway mimicking the natural infection
308 fully following the criteria of OIE standards.

309 *E. carinicauda* is one of the important economic local crustacean distributing in Yellow Sea and
310 Bohai Sea, which has been cultivated broadly in Jiangsu, Zhejiang, Shandong, and Liaoning Provinces
311 of China [11,12]. It has been reported that *E. carinicauda* is a natural host of some viral pathogens,
312 such as WSSV [25] and CMNV [26]. *E. carinicauda* was also considered as a potential model animal
313 for researching shrimp viral pathogens [27].

314 In order to investigate the susceptibility of *E. carinicauda* to SHIV, *E. carinicauda* were
315 experimentally challenged with SHIV *per os* and intramuscular injection, following the OIE standards.
316 After three days post challenge, infected prawns from both PO and IM groups displayed same clinical
317 symptoms, including debility, empty guts and stomach, pale hepatopancreas, slight whitish
318 hematopoietic tissue, and mortalities. Much higher doses of SHIV were detected in the moribund and
319 died prawns in the intermuscular injection group than those in the *per os* group. The significant
320 difference in viral dose may due to that injection of SHIV caused extensive and synchronous infection
321 in different target cells. The clinical signs observed in *E. carinicauda* were similar to that of *P. vannamei*
322 affected by SHIV in the study of Qiu et al. [9] and also similar to that of lethargy, anorexia, and
323 mortality affected by CQIV [8]. According to the results of our challenge test, in the duration of 20
324 days, cumulative mortalities of *E. carinicauda* were (76.7±18.3)% and (50.0±26.5)% in groups of im and
325 *per os*, respectively. Based on the pathogenic model resulted from nonlinear regression, the bioassay
326 revealed that *E. carinicauda* showed some tolerant to the infection with SHIV *per os* challenge
327 mimicking natural infection, which caused only (60.1±6.3)%-fold mortality within (1.45±0.35)-fold
328 time spending at (17.2±14.0)%-fold slow instant speed comparing with the direct im challenge. The
329 SHIV positive survival prawns in *per os* challenged group possessed viral loads at (3.57±3.42)×10²
330 copies/ng-DNA, which were about 100 folds lower than that detected in died prawns via im challenge.
331 Previous studies showed that mortalities of experimental *P. vannamei*, *C. quadricarinatus* and *Pr. clarkii*
332 challenge with SHIV or CQIV reached 100% [8,9]. These results indicated that *E. carinicauda* were
333 likely resistant to SHIV to some degrees, which may provide a object for future study on mechanism
334 and breeding of SHIV resistance. As *E. carinicauda* is a broadly distributing local species, the partial
335 resistance of the ridgetail white prawn to SHIV may also provide a possible reservoir of the virus
336 after the virus transports to the species in the area of the Yellow Sea, the Bohai Sea, and the East China
337 Sea.

338 Positive tests of TaqMan qPCR and ISDL provided further evidences to the infection of *E.*
339 *carinicauda* by SHIV. According to the results of ISDL, positive detection signals were detected in the
340 hepatopancreatic sinus, hematopoietic tissue and cuticular epithelium of infected *E. carinicauda*.
341 Previous studies showed that cuticular epithelium is a major target tissue of WSSV infection [25,28].
342 However, cuticular epithelium of *P. vannamei* is not a susceptible tissue to SHIV infection. Our results

343 showed difference in the tissue tropism between *E. carinicauda* and *P. vannamei* to SHIV infection.
344 ISDL [18] is a highly sensitive and time-saving method, compared to normal *in situ* hybridization
345 (ISH). In addition, the histopathological examination of diseased *E. carinicauda* were consistent or
346 similar to that previously reported in *P. vannamei*, *C. quadricarinatus*, and *Pr. clarkii* [8,9]. Moreover,
347 in this study, massive SHIV virions with dense cores, characterized by icosahedral and ~150 nm in
348 diameter, consistent with the report of Qiu et al. [9], were observed in hemocytes of hepatopancreatic
349 sinus and gills of *E. carinicauda* from IM and PO groups. The virions primarily existed in cytoplasm
350 of hemocytes and branchial cells. Additionally, SHIV virions were also observed in pereopods,
351 muscles and uropods of *E. carinicauda* from the IM group. These results expanded the knowledge of
352 tissue tropism of SHIV. Different infection paths of SHIV, including intramuscular injection and *per*
353 *os* infection, contributed to significant differences on mortality and viral loads in *E. carinicauda*
354 between the IM group and the PO group.

355 Taken together, the results of clinical observation, molecular biological diagnosis, histological
356 examination, and TEM observation supported that *E. carinicauda* is a newly demonstrated susceptible
357 species to SHIV, following the criteria for listing species as susceptible to infection with a specific
358 pathogen developed by the OIE [10]. Currently, there was no naturally diseased SHIV case of *E.*
359 *carinicauda* reported in farm or in sea area. As *E. carinicauda* has local economic importance,
360 Biosecurity strategies [29,30] should be taken into account on the risk that SHIV can causes disease
361 in *E. carinicauda* and the risk that the species becomes a possible reservoir of SHIV. It also should not
362 be ignored that *E. carinicauda* showed some degree of tolerance to infection with SHIV, especially *per*
363 *os* challenge mimicking natural pathway.

364 **Supplementary Materials:** The following are available online at www.mdpi.com/xxx/s1, Figure S1: Positive data
365 of SHIV qPCR detection within 40 cycles in IM and PO groups.

366 **Author Contributions:** Conceptualization, J.H. and X.C.; Formal analysis, X.C.; Methodology, X.C., H.W., L.Q.,
367 P.Z., and X.D.; Writing-Original Draft Preparation, X.C.; Writing-Review & Editing, J.H., H.W., F.L. and X.C.;
368 Supervision, J.H.; Project administration, J.H. and X.C.; Funding acquisition, J.H.

369 **Funding:** This research was financially supported by the Marine S&T Fund of Shandong Province for Pilot
370 National Laboratory for Marine Science and Technology (Qingdao) (2018SDKJ0502-3), the Pilot National
371 Laboratory for Marine Science and Technology (Qingdao) (QNL201706), the China ASEAN Maritime
372 Cooperation Fund Project (2016-2018) and the China Agriculture Research System (CARS-48).

373 **Acknowledgments:** We are grateful to all the laboratory members for their technical advice and helpful
374 discussions.

375 **Conflicts of Interest:** The authors declare no conflict of interest. The funders had no role in the design of the
376 study; in the collection, analyses, or interpretation of data; in the writing of the manuscript, and in the decision
377 to publish the results.

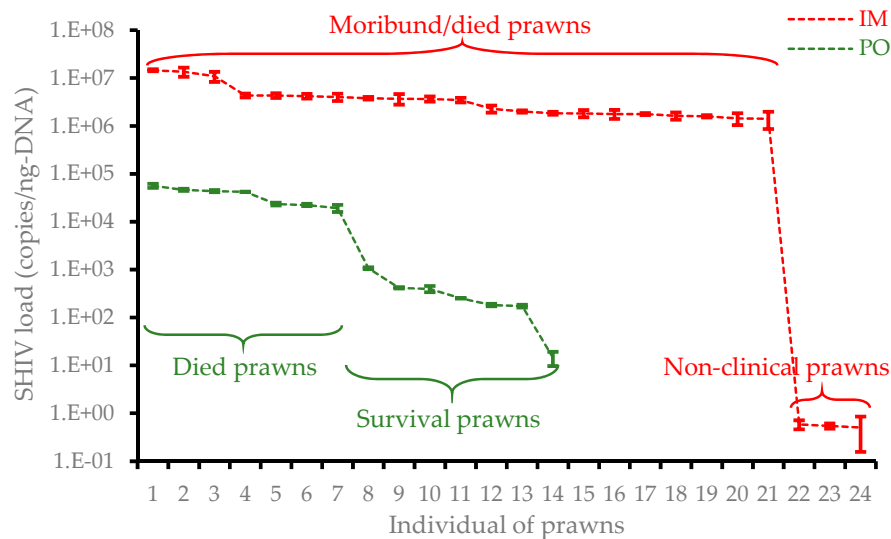
378

379 References

- 380 1. Jun, K.; Kazuhiro, N. Megalocytiviruses. *Viruses* **2012**, *4*(4), 521-538, doi: 10.3390/v4040521.
- 381 2. Chinchar, V.G.; Yu, K.H.; Jancovich, J.K. The Molecular biology of Frog virus 3 and other Iridoviruses
382 infecting cold-blooded vertebrates. *Viruses* **2011**, *3*(10), 1959-1985, doi: 10.3390/v3101959.
- 383 3. Chinchar, V.G.; Hick, P.; Ince, I.A.; Jancovich, J.K.; Marschang, R.; Qin, Q.W.; Subramaniam, K.; Waltzek,
384 T.B.; Whittington, R.; Williams, T.; Zhang, Q.Y. ICTV virus taxonomy profile: Iridoviridae. *J. Gen. Virol.*
385 **2017**, *98*(5), 890-891, doi: 10.1099/jgv.0.000818.
- 386 4. Montanie, H.; Bonami, J.R.; Comps, M. Irido-like virus infection in the crab *Macropipus depurator* L.
387 (Crustacea, Decapoda). *J Invertebr Pathol* **1993**, *61*(3), 320-322. doi: 10.1006/jipa.1993.1060.
- 388 5. Lightner, D.V.; Redman, R.M. A putative iridovirus from the penaeid shrimp *Protrachypene precipua*
389 Burkenroad (Crustacea Decapoda). *J Invertebr Pathol* **1993**, *1*, 107-109.
- 390 6. Miao, H.Z.; Tong, S.L.; Xu, B.; Jiang, M.; Liu, X.Y. Viral and Pathological observation in cultured lymphoid
391 tissues of shrimp *Penaeus chinensis*. *J. Fisheries of China* **1999**, *2*, 169-173. doi: 10.1006/jipa.1993.1084.

- 392 7. Tang, K.F.J.; Redman, R.M.; Pantoja, C.R.; Groumellec, M.L.; Duraisamy, P.; Lightner, D.V. Identification
393 of an iridovirus in *Acetes erythraeus* (Sergestidae) and the development of in situ hybridization and PCR
394 method for its detection. *J Invertebr Pathol* **2007**, *96*(3), 255-260, doi: 10.1016/j.jip.2007.05.006.
- 395 8. Xu, L.M.; Wang, T.; Li, F.; Yang, F. Isolation and preliminary characterization of a new pathogenic
396 iridovirus from redclaw crayfish *Cherax quadricarinatus*. *Dis Aquat Organ* **2016**, *120*(1), 17-26, doi:
397 10.3354/dao03007.
- 398 9. Qiu, L.; Chen, M.M.; Wan, X.Y.; Li, C.; Zhang, Q.L.; Wang, R.Y.; Cheng, D.Y.; Dong, X.; Yang, B.; Wang,
399 X.H.; Xiang, J.H.; Huang, J. Characterization of a new member of *Iridoviridae*, Shrimp hemocyte iridescent
400 virus (SHIV), found in white leg shrimp (*Litopenaeus vannamei*). *Sci Rep-Uk* **2017**, *7*(1), doi: 10.1038/s41598-
401 017-10738-8.
- 402 10. OIE. Chapter 1.5 Criteria for listing species as susceptible to infection with a specific pathogen. In *Aquatic*
403 *Animal Health Code*, 21st Edition, World Organisation for Animal Health, **2018**, Paris, ISBN: 978-92-95108-
404 69-1, http://www.oie.int/index.php?id=171&L=0&htmfile=chapitre_criteria_species.htm
- 405 11. Xu, W.; Xie, J.; Shi, H.; Li, C. Hematodinium infections in cultured ridgetail white prawns, *Exopalaemon*
406 *carinicauda*, in eastern China. *Aquaculture* **2010**. *300*(1-4), 25-31, doi: 10.1016/j.aquaculture.2009.12.024.
- 407 12. Wang, X.Q.; Yan, B.L.; Ma, S.; Dong, S.L. Study on the biology and cultural ecology of *Exopalaemon*
408 *carinicauda*. *Shandong Fisheries* **2005**. *08*, 21-23.
- 409 13. OIE. Manual of Diagnostic Tests for Aquatic Animals, 7th Edition. World Organisation for Animal Health,
410 **2016**, ISBN 978-92-9044-887-7, <http://www.oie.int/standard-setting/aquatic-manual/access-online/>,
411 accessed on 10 Jan, 2019.
- 412 14. Li, X.P.; Wan, X.Y.; Xu, T.T.; Huang, J.; Zhang, Q.L. Development and validation of a TaqMan RT-qPCR for
413 the detection of convert mortality nodavirus (CMNV). *J Virol Methods* **2018**. *262*, 65-71, doi:
414 10.1016/j.jviromet.2018.10.001.
- 415 15. Qiu, L.; Chen, M.M.; Wan, X.Y.; Zhang, Q.L.; Li, C.; Dong, X.; Yang, B.; Huang, J. Detection and
416 quantification of shrimp hemocyte iridescent virus by TaqMan probe based real-time PCR. *J Invertebr Pathol*
417 **2018**, *154*, 95-101, doi: 10.1016/j.jip.2018.04.005.
- 418 16. Huang, J.; Song, X.L.; Yu, J.; Zhang, L.J. The components of an inorganic physiological buffer for *Penaeus*
419 *chinensis*. *Methods Cell Sci* **1999**. *21*(4), 225-230.
- 420 17. Bell, T.A.; Lightner, D.V. A Handbook of Normal Penaeid Shrimp Histology. **1988**, World Aquaculture
421 Society, Baton Rouge, Louisiana, USA, ISBN 0-935868-37-2.
- 422 18. Jitrakorn, S.; Arunrut, N.; Sanguanrut, P.; Flegel, T.W.; Kiatpathomchai, W.; Saksmerprom, V. *In situ* DIG-
423 labeling, loop-mediated DNA amplification (ISDL) for highly sensitive detection of infectious hypodermal
424 and hematopoietic necrosis virus (IHHNV). *Aquaculture* **2016**. *456*, 36-43, doi:
425 10.1016/j.aquaculture.2016.01.023.
- 426 19. Lightner, D.V. A Handbook of Shrimp Pathology and Diagnostic Procedures for Disease of Cultured
427 Penaeid Shrimp. **1996**, World Aquaculture Society, Baton Rouge, USA, ISBN 0-962452-99-8.
- 428 20. Graham, L.; Orenstein, J.M. Processing tissue and cells for transmission electron microscopy in diagnostic
429 pathology and research. *Nat Protoc* **2007**. *2*(10), 2439-2450, doi: 10.1038/nprot.2007.304.
- 430 21. Panphut, W.; Senapin, S.; Sriurairatana, S.; Withyachumnarnkul, B.; Flegel, T.W. A novel integrase-
431 containing element may interact with Laem-Singh virus (LSNV) to cause slow growth in giant tiger shrimp.
432 **2011**. *7*(1), 18-??, doi: 10.1186/1746-6148-7-18.
- 433 22. Qiu, L.; Dong, X.; Wan, X.Y.; Huang, J. Analysis of iridescent viral disease of shrimp (SHID) in 2017. In
434 *Analysis of Important Diseases of Aquatic Animals in China in 2017* (in Chinese). Fishery and Fishery
435 Administration Bureau under the Ministry of Agriculture and Rural Affairs, National Fishery Technical
436 Extension Center, Eds.; China Agriculture Press, Beijing, 2018; pp. 187-204, ISBN 978-7-109-24522-8.
- 437 23. Qiu, L.; Chen, X.; Zhao, R.H.; Li, C.; Gao, W.; Zhang, Q.L.; Huang, J. First description of a natural infection
438 of Shrimp hemocyte iridescent virus in cultured giant freshwater prawn, *Macrobrachium rosenbergii*. *Viruses*
439 (under review).
- 440 24. Kun, P.C.; Fang, Y.H.; Tian, W.T.; Feng, Y.; Ming, C.J. Study of *Cherax quadricarinatus* iridescent virus in
441 two crabs. *J Applied Oceanography* **2017**, *1*, 82-86, doi: 10.3969/j.issn.2095-972.2017.01.010.
- 442 25. Lei, Z.W.; Huang, J.; Shi, C.Y.; Zhang, L.J.; Yu, K.K. Investigation into the hosts of White spot syndrome
443 virus (WSSV). *Oceanologia et Limnologia Sinica* **2002**, *33*(3), 250-258.

- 444 26. Liu, S.; Li, J.T.; Tian, Y.; Wang, C.; Li, X.P.; Xu, T.T.; Li, J.; Zhang, Q.L. Experimental vertical transmission
445 of covert mortality nodavirus in *Exopalaemon carinicauda*. *J Gen Virol* **2017**, *98*(4), 652-661, doi:
446 10.1099/jgv.0.000731.
- 447 27. Zhang, J.; Wang, J.; Gui, T.; Sun, Z.; Xiang, J. A copper-induced metallothionein gene from *Exopalaemon*
448 *carinicauda* and its response to heavy metal ions. *Int J Biol Macromol* **2014**, *70*(8), 246-250, doi:
449 10.1016/j.ijbiomac.2014.06.020.
- 450 28. Huang, J.; Song, X.L.; Yu, J.; Yang, C.H. Baculoviral hypodermal and hematopoietic necrosis -- study on
451 the pathogen and pathology of the explosive epidemic disease of shrimp. *Marine Fisheries Research* (in
452 Chinese with English abstract) **1995**, *16*(1), 1-10.
- 453 29. Huang, J.; Zeng, L.B.; Dong, X.; Liang, Y.; Xie, G.S.; Zhang, Q.L. Trend Analysis and Policy
454 Recommendation on Aquatic Biosecurity in China. *Engineering Sciences* (in Chinese with English abstract)
455 **2016**, *18*(03), 15-21, <http://engineering.ckcest.cn/cjes/CN/abstract/abstract18019.shtml>.
- 456 30. Huang, J.; Dong, X.; Zhang, Q.L.; Wan, X.Y.; Xie, G.S.; Yang, B.; Wang, H.L.; Yang, Q.; Xu, H.; Wang, X.H.
457 Emerging diseases and biosecurity strategies for shrimp farming. In #We R Aquaculture, AQUA 2018, The
458 World Aquaculture Society, Montpellier, France, Aug. 25-29, 2018, pp. 356,
459 <http://www.was.org/Meetings/ShowAbstract.aspx?Id=104234>.
- 460
461



462

463

Figure S1. Positive data of SHIV qPCR detection within 40 cycles in IM and PO groups.